Evolution study of photo-synthesized gold nanoparticles by spectral deconvolution model: a quantitative approach

Chung-Sung Yang,* Mong-Shian Shih and Fang-Yi Chang

Received (in Montpellier, France) 21st November 2005, Accepted 23rd February 2006
First published as an Advance Article on the web 17th March 2006
DOI: 10.1039/b516465f

During the monitoring of the evolution of Au nanoparticles photo-synthesized *via* a conventional long-wave UV-visible irradiation (200 nm $< \lambda <$ 600 nm) in an aqueous solution, two independent growth progresses of nanocrystals were observed. The first growth progress of nanoparticles was initiated between 90 and 96 h (D-5 samples) and mainly evolved to 10–25 nm in diameter. The second growth progress occurred between 136 and 144 h (D-7 samples) and grew mostly to 3–5 nm in diameter. In the surface plasmon absorption spectra of these samples, a continuous blue-shift of λ_{max} from 543 nm (D-8 samples) to 525 nm (D-14 samples) was observed. A spectral deconvolution model was employed to quantitatively investigate the peak area variation of the component peaks comprising the absorption spectra. It can be concluded from the deconvoluted data of the peak areas for the component peaks that the blue-shift phenomenon is due to the contribution of the second growth progress of Au nanoparticles. If the second growth progress no longer develops, the blue-shift phenomenon of the surface plasmon absorption peak is found to cease.

1 Introduction

Chemical reduction methods have been employed for the past decade as common ways to synthesize colloidal metal nanoparticles, including alcohol reduction,[1–3] hydrogen reduction,[4,5] and sodium borohydride reduction.[6–8] Meanwhile, other developed reduction methods, such as electrochemical,[9,10] photochemical,[11,12] and sonochemical[13–15] reduction methods have been used to a smaller extent in the synthesis of noble metal nanoparticles, especially gold nanoparticles.[13,14] Noble metal nanoparticles have attracted intensive attention from researchers in the optoelectronic and the catalytic fields because the unusual optical properties and catalytic activities of noble metal nanoparticles can be boosted dramatically by variation of particle size or modification of the particle shape.[16,17] For example, colloidal gold nanorods exhibit an enhancement of 10^6 in the yield of photoluminescence as compared to bulk Au metal.[18] Recently, laser-induced syntheses and morphological variation for noble metal nanoparticles have been reported.[16] Silver nanoparticles (diameter (d) = 40–60 nm) with a surface plasmon absorption band wavelength maximum (λ_{max}) around 420 nm, were decomposed to about 5 nm after a 355 nm laser irradiation.[19] A blue-shift in absorption spectrum was recorded and accompanied by a narrowing of the absorption band.[19] If the intensity of the irradiation is low, a morphology change from spherical to tetrahedral shape is observed.[20] The size fusion, fragmentation, and shape transformation due to the laser-induced method has been well studied in Au nanoparticles.[4,19,21] Nevertheless, the studies on the relationships among the irradiation source, particle fragmentation and morphology transformation of Au nanocrystals by the photo-induced route are scant.[22] We used a conventional UV-visible irradiation (λ = 200–600 nm) method to investigate the crystal growth and the size variation of Au nanoparticles. During the monitoring of the evolution progress of the Au nanoparticles, we found that the λ_{max} of the surface plasmon absorption peak for Au nanoparticles varied (blue-shift) with the evolution time of the nanoparticles. Two groups of nanoparticles with a large difference in size distribution were observed in the final products. One group lies mainly in the range 10–25 nm in diameter and the other group is in the 3–5 nm diameter range. In this study, we employ a spectral deconvolution model to quantitatively investigate the size variation of the Au nanoparticles during their evolution progress. This model can provide us with a quantitative peak area change of the component peaks that comprise the entire surface plasmon absorption peak, which is a very convenient way to study the evolution mechanism of the nanoparticles.

Department of Applied Chemistry, National Chia Yi University, Chia Yi, 60004 Taiwan, R.O.C. E-mail: csyang@mail.ncyu.edu.tw; Fax: +(886)-5-2717901; Tel: +(886)-5-2717962

2 Experimental

2.1 Chemicals

Sodium tetrachloroaurate(III) dihydrate ($NaAuCl_4 \cdot 2H_2O$, 99%), and sodium dodecyl sulfate (SDS) were purchased from Aldrich and J. T. Baker, respectively. Secondary de-ionized water was used without any further purification. HPLC grade methanol, and reagent grade ethanol were obtained from Aldrich, and used as supplied.

2.2 Synthesis and characterization

The starting reagents $NaAuCl_4$ (1 mM) and SDS (8 mM) were dissolved completely in 50 mL of secondary de-ionized water

in a Schlenk-line N_2 atmosphere. The solution was a clear golden–yellow color before the irradiation by UV-visible light. The photo-synthesis of Au nanoparticles was carried out by a Perkin Elmer Lambda 40 spectrophotometer, equipped with a dual-beam system; halogen lamp (visible light region) and deuterium lamp (UV region). Each sample (4 mL) was irradiated continuously five cycles a day by the dual-beam source, λ = 200–600 nm. Each cycle includes three steps: (a) initially samples were irradiated with visible light (λ = 600–327 nm) for 140 s. (b) Second, samples were irradiated by ultraviolet light (λ = 327–200 nm) for 60 s. (c) Finally, samples were left in the dark for 100 s. At step (c), samples were slowly stirred or shaken for about 90 s before the start of the next irradiation cycle. After the five cycles, samples were then kept at room temperature prior to the next irradiation time. In the first four days, the color of the samples did not change. On the fifth day, however, the color of the samples started to gradually turn to purple–red (denoted as D-5, *ca.* 92–96 h after the first irradiation cycle). This change of color is an indicator confirming that the Au nanoparticles have been successfully photo-synthesized.[22,23] The size variation of the nanoparticles was measured by transmission electron microscopy (TEM) and qualitative analysis by energy dispersive spectra (EDS) from TEM. The photo-irradiation was performed continuously for 21 days, and the final products (D-21) show a deep purple–red color without any precipitation. All samples were stable in air for more than 6 months.

For the experiments of sonochemical synthesis of Au nanoparticles, the same concentration of $NaAuCl_4$ (1 mM) and SDS (8 mM) aqueous solutions were prepared. The output powder of the sonicator (Misonix 3000) was set at 18 W for two continuous 30 min sonication cycles at room temperature. A water-bath was employed to prevent any temperature rise caused by the sonication to the sample. The color of the solution changed from a clear golden–yellow to a purple–red after the completion of sonication process. These solutions were then treated by the same UV-visible irradiation cycle as for the photo-synthesized samples.

Transmission electron microscopy (TEM) images and high-resolution TEM (HR-TEM) images were collected on a JOEL 2010 HR microscope at 200 kV accelerating voltage. Samples were prepared by evaporation of the colloidal solution onto a 200 mesh Cu grid. TEM energy dispersive spectra (EDS) were acquired on a JOEL 2010HR. UV and visible spectra were collected on a Perkin Elmer Lambda 40 spectrophotometer. Fourier transform infrared (FT-IR) spectra were recorded on a Thermo Nicolet Avatar 360 spectrophotometer. All spectra were recorded at room temperature.

3 Results and discussion

3.1 Synthesis of Au nanoparticles

3.1.1 Photo-synthesis route. In the plasmon absorption spectra for the as-prepared starting reagent solutions (denoted as D-1) *i.e.* the initial samples, a sharp peak in the range 280–440 nm with λ_{max} at 300 nm is observed, as shown in Fig. 1. This absorption peak is generally attributed to the absorption of Au^{3+} cations in the UV region.[23] In the D-3 samples, (after 48 h irradiation), the peak centered at 300 nm is still the only absorption observed in the spectrum. The colors of the samples remained unchanged from samples D-1 to D-3.

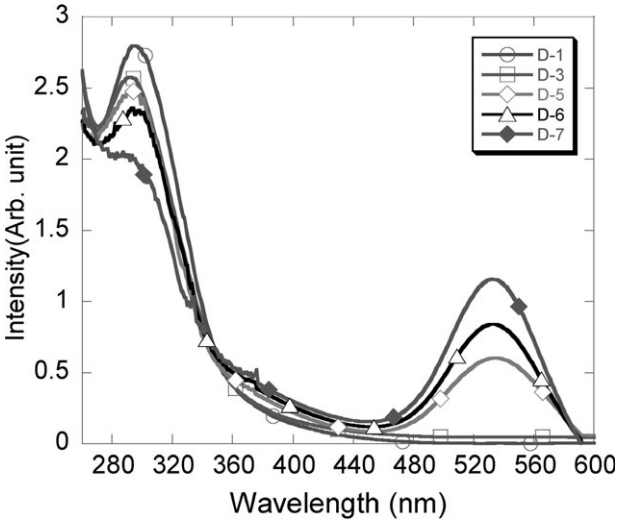

Fig. 1 Surface plasmon absorption spectra showing variation with irradiation time. In the D-1 samples (starting reagent), up to D-3 (at 48 h), a peak with λ_{max} at 300 nm is observed, which is generally attributed to the absorption of Au^{3+} cations. On the fifth day (D-5), a new peak at 548 nm is evident in addition to the λ_{max} = 300 nm peak, which confirms the existence of Au nanoparticles. On the seventh day (D-7), the intensity of the 548 nm peak is doubled, at the expense of the decrease of the intensity of the 300 nm peak.

On the fifth day (D-5), the color of the samples turned gradually to a purple–red within 2–3 h, (after 92–96 h). A new peak (λ_{max} at 548 nm), in the range 460–600 nm, is observed in the absorption spectrum for the D-5 samples in addition to the original peak (λ_{max} at 300 nm). The peak centered at 548 nm is typically assigned to the existence of Au nanoparticles ($d >$ 5 nm) that usually changes the color of the colloidal solution to a purple–red.[22–24] In the surface plasmon absorption spectra for the D-7 (144 h) samples, the intensity of the 548 nm peak was doubled, compared to that of D-5 samples, at the expense of a decreased intensity of the 300 nm peak. The TEM images for the D-5 and D-7 samples are shown in Fig. 2(a)–(d). Some tiny crystalline seeds, $d <$ 1 nm, can be clearly seen in the enlarged views of the D-5 and D-7 images. The high-resolution TEM micrograph (Fig. 2(e)) for one of the D-7 nanocrystals (in the correct orientation to show the *d*-spacings of the lattice fringes: 1.45 Å) is consistent with the {220} crystal plane of cubic-structured Au. Fig. 2(f) shows a histogram of the size distribution derived from four TEM images that were taken from four different samples. The average size distribution of the nanoparticles is 6.9 ± 1.8 nm (D-5 samples) and 8.2 ± 1.9 nm (D-7 samples). If the samples are irradiated for a further seven days (D-14), the intensity of the surface plasmon absorption peak increases only slightly. However, an obvious blue-shifting was observed in the absorption spectra. The λ_{max} of the absorption peak shifted from 548 nm (D-7) to 545 nm (D-8), 535 nm (D-10, 216 h), and finally reached 523 nm (D-14, 312 h), as shown in Fig. 3. The intensity of the absorption peak is related to the oscillator strength of the

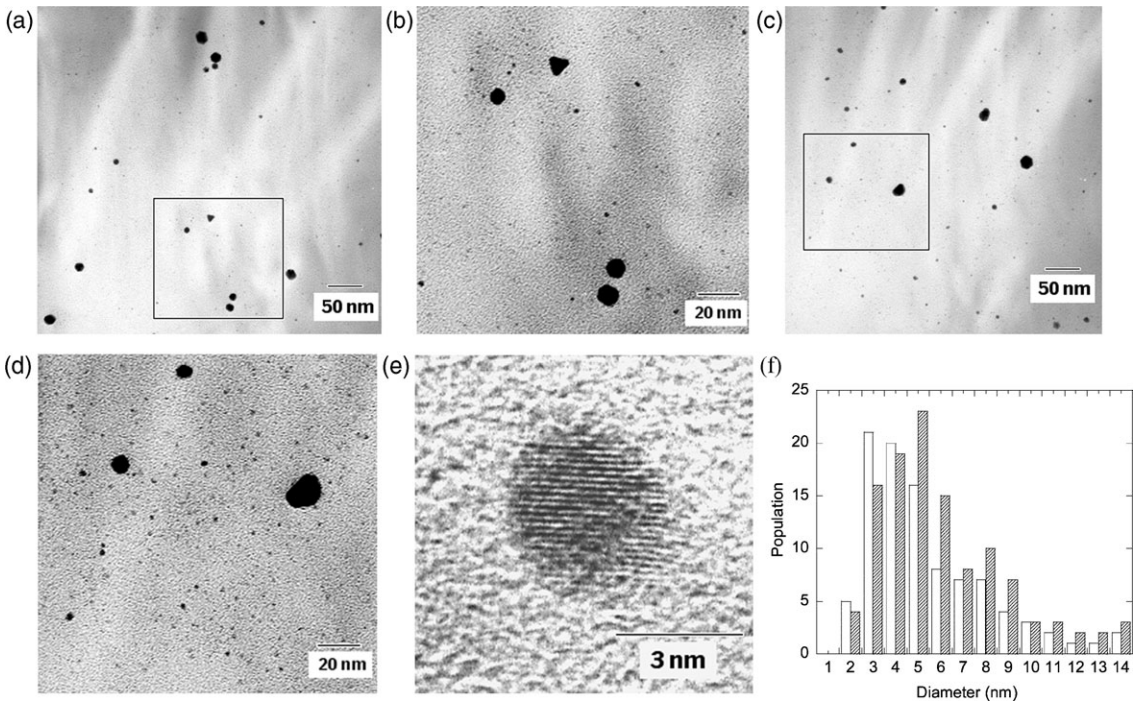

Fig. 2 TEM images for (a), (b) D-5 samples and (c), (d) D-7 samples. Some tiny crystalline seeds, $d < 1$ nm, can be clearly seen in the expansions of the D-5 and D-7 images. (e) High-resolution TEM micrograph for one of the D-7 nanocrystals in the correct orientation to show the *d*-spacings of the lattice fringes (1.45 Å) which is consistent with the {220} crystal plane of cubic-structured Au (JCPDS 04-0784). (f) Histogram of the size distribution derived from TEM images. The size data for D-5 are indicated by blank columns and those for D-7 are indicated by diagonal lines. The average size distribution of the nanoparticles is 6.9 ± 1.8 nm (D-5 samples) and 8.2 ± 1.9 nm (D-7 samples).

surface plasmon band and the concentration of the nanoparticles.[24] IR spectra confirmed that the surface termination agent for all samples is similar, either SDS or derived species. Therefore, the only possible factor that can affect the intensity

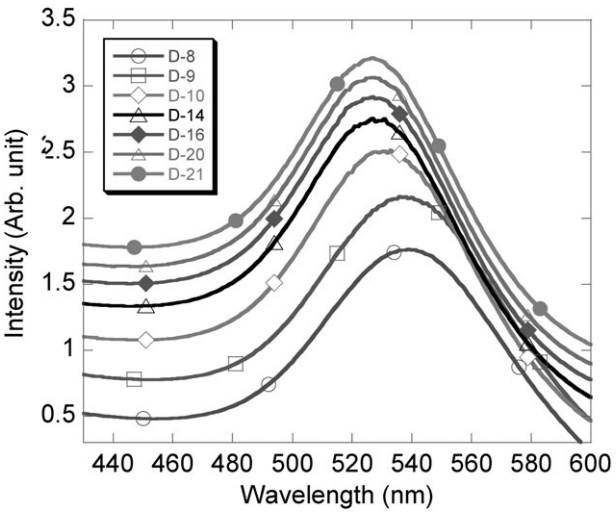

Fig. 3 An obvious λ_{max} blue-shifting of the surface plasmon absorption peak from 545 nm (D-8) to 535 nm (D-10) and finally to 523 nm (D-14, at 312th h) is observed. Whilst blue-shifting is clearly observed the intensity of absorption peak increases only slightly from D-8, D-10 to D-14. If the evolution is allowed to continue for another 7 days, from D-15 to D-21 (at the 480th h), the blue-shift, from 523 nm (D-16) to 521 nm (D-21), is negligible.

of the 548 nm peaks is the concentration of mature Au nanoparticles (nanoparticles with stable surface-to volume size).[25] A rational explanation as why the intensity of the 548 nm peak of the D-7 (at after 144 h) approaches a maximum and starts a continuous blue-shift of the surface plasmon absorption peak is the fact that the first crystal growth of Au nanoparticles reaches an intermediate stable size region, $d = 8.2 \pm 1.9$ nm after seven days and then shows a slower growth rate.[25] Nevertheless, the newly available crystalline seeds, $d < 1$ nm, quickly grow toward the stable surface-to-volume region after cross over the activation energy barrier (E_a), which initiates the second crystal growth progress[25] and starts a blue-shift of the surface plasmon absorption peak.

If the evolution is allowed to continue for another 7 days, from D-15 to D-21 (termination at 480 h), then the blue-shift distance, from 523 nm (D-16) to 521 nm (D-21), (Fig. 3), is within the instrumental derivation range. The data implied that the second growth mechanism of Au nanoparticles slows down dramatically after D-14.

In the TEM images of the D-10 and D-14 samples, as shown in Fig. 4, a large number of small nanoparticles is observed, in addition to the larger ones. The diameters of these small nanoparticles are in the size of 3–5 nm, and the larger ones reach a diameter of 10–20 nm. The 3–5 nm small size nanoparticles were not found in the D-5 and D-7 samples and their appearance confirms the existence of the second crystal growth progress. In the micrograph for the final products, (D-21 sample), the sizes of the nanoparticles are categorized into

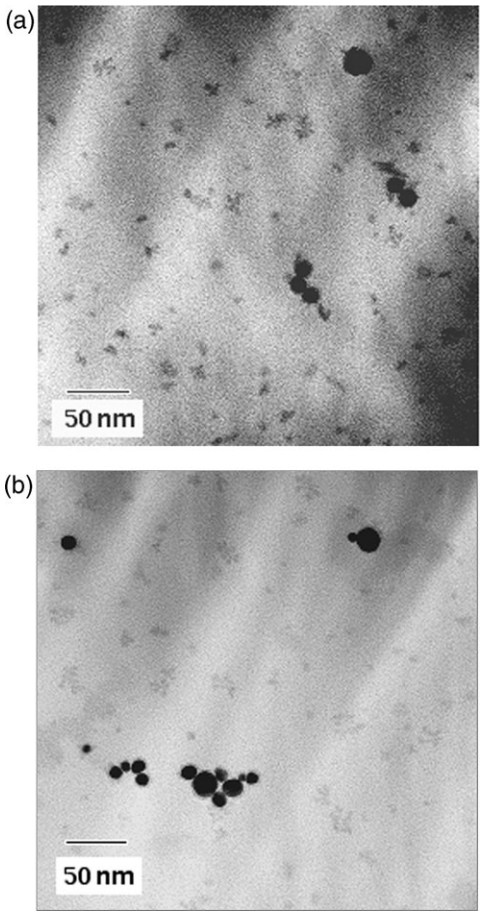

Fig. 4 TEM images for (a) D-10 and (b) D-14 samples. A large number of tiny nanoparticles is observed, in addition to the larger ones. These small size nanoparticles were not found in the D-5 and D-7 samples. The diameters of these small nanoparticles are in the size range 3–5 nm, while the larger ones reach a size of 10–20 nm (diameter).

two groups, one from 3 to 5 nm and the other from 10 to 25 nm, which are similar to the results of the D-10 and D-14 samples. Most of the particles in the final products are spherical or nearly spherical. Only very few trigonal or tetragonal shaped particles were found. The large-scale photo-induced morphology conversion from spherical shape into tetragonal and triangular shaped nanoparticles is not evident in this case, but the aggregation of nanoparticles is obvious.

This is the first report of the appearance of the blue-shift phenomenon in the surface plasmon absorption peak during the monitoring of the growth progress of photo-synthesized Au nanoparticles. Although, Au nanoparticles do not possess a band gap between the valence and conduction band, it is well known that smaller size Au nanoparticles will exhibit higher absorption energy in plasmon absorption spectra.[24,26] When free electrons move into the intraband, the oscillation modes of electrons explicitly depend on the particle size.[26] If the size of the nanoparticles decreases, then the bandwidth will also decrease. Consequently, the plasmon absorption maximum will be shifted to a shorter wavelength, *i.e.* blue-shifting, because the oscillation frequencies will be increased in a smaller space.[24,26,27] The reason for the broadening peak width of the plasmon absorption peak in this case is because of a superposition of all the contributing multiple oscillations peaking at different energies due to the size distribution of the nanoparticles.[24,26] Some reports have indicated that the broadening of the surface plasmon absorption peak is ascribed to retardation effects.[26] However, in this study, we very carefully examined the λ_{max} blue-shifting of the surface plasmon absorption peak during the Au nanoparticles evolution progress. We confirmed that a larger energy is required to move an electron into the intraband of the smaller size Au nanoparticles compared with that of the larger size ones.

3.1.2 Sonolytic synthesis route. The sonochemical synthesized Au nanoparticles was prepared according to literature.[28] The yield of the product was quite high and the size of the as-prepared nanoparticles varied mainly from 6 to 12 nm in diameter, as shown in Fig. 5(a). These as-prepared samples were then irradiated by the same irradiation source used for the photo-synthesis samples in order to examine the light induced fragmentation effect. Interestingly, these samples

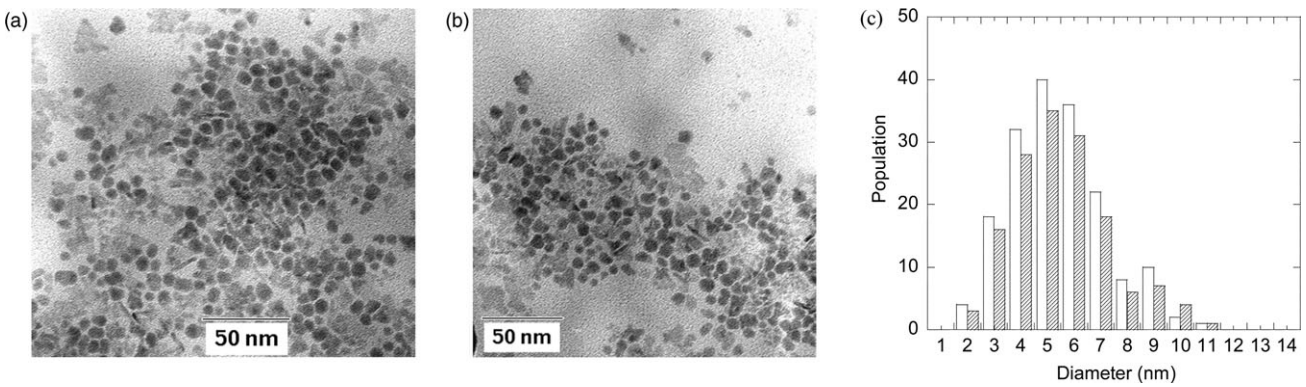

Fig. 5 TEM images for the sonochemically synthesized Au nanoparticles. (a) The yield of the product was quite high and the size of the as-prepared nanoparticles varied mainly in the range 6–12 nm in diameter. (b) In this TEM image, no evidence for photolysis decomposition or photo-fusion phenomenon of Au nanoparticles was found, after a 21-day UV-Vis irradiation cycle was applied on the as-prepared sample. (c) Histogram of the size distribution derived from TEM images. The size data for the as-prepared sample are indicated by blank columns and those for the after-photo-irradiation sample are indicated with diagonal lines. The average size distribution of the nanoparticles is 8.5 ± 1.1 nm (as-prepared) and 8.7 ± 1.9 nm (after-photo-irradiation).

can survive a 21-day UV-Vis irradiation cycle without any obvious particle decomposition or fusion, as shown in Fig. 5(b). The histogram of the size distribution derived from four TEM images taken from two different samples is provided in Fig. 5(c). The average size distribution of the nanoparticles is 8.5 ± 1.1 nm (as-prepared) and 8.7 ± 1.9 nm (after photo-irradiation). The λ_{max} shift distance of the surface plasmon absorption peak between the before UV-irradiated (as-prepared) and after UV-irradiated samples is very small ($\Delta\lambda_{max}$ = 3 nm, *i.e.* λ_{max} shifting from 555 nm to 552 nm). The result supports the reasoning that the appearance of smaller nanoparticles, those with diameters in the range 3–5 nm in D-10 and D-14 samples, is not related to the photolysis of larger nanoparticles ($d > 5$ nm) into small fragments ($d < 5$ nm). The appearance of these smaller size nanoparticles is more likely evolved from another nanocrystal growth mechanism.

3.2 Mechanism for the evolution of photo-synthsized Au nanoparticles

We propose a time-evolved, kinetic-dependent mechanism based on the phenomena observed in monitoring the crystal growth of Au nanoparticles photo-synthesized by a conventional UV-visible irradiation. In the initial step, the Au cations are reduced by SDS under the UV-Vis irradiation.[28] The reduction progress depends highly on the dissociation rate of free radicals from SDS by UV-Vis irradiation.[28] The progress is then followed by the competition between nucleation of atoms into crystalline seeds and decomposition of crystalline seeds back to neutral atoms.[25] The absorption peak intensity of Au cations (λ_{max} = 300 nm) decreases as the reduction progress of Au cations proceeds. In this evolution state, the sizes of these crystalline seeds are different. The larger crystallites are those who survive early from the competition and grow toward the stable surface-to-volume region after crossing over the activation energy barrier (E_a). On the other hand, the smaller seeds are still in competition or even decompose back to neutral atoms. The competition mechanism is indicated in the following equations:

$$(1)\ (m+n)\,H_3(CH_2)_{11}OSO_3Na +))))^{(a)} \rightarrow m\,R^{\bullet\ (b)} + m\,^{\bullet}R'OSO_3Na^{(c)} + n\,CH_3(CH_2)_{11}OSO_3Na$$

(*a*))))) = UV-Vis irradiation energy
(*b*) $^{\bullet}R$ = $^{\bullet}CH_3$ or $^{\bullet}C_2H_5$
(*c*) $^{\bullet}R'\ OSO_3Na$ = $^{\bullet}(CH_2)_{11}OSO_3Na$ or $^{\bullet}(CH_2)_{10}OSO_3Na$

$$(2)\ a\,Au^{3+} + m\,^{\bullet}R \rightarrow (Au)_x + (Au)_y + (Au)_z + (a-x-y-z)\,Au^{3+} + (m-x-y-z)\,^{\bullet}R$$

* (size of seed: $(Au)_x < (Au)_y < (Au)_z$)

$$(3)\ (i)\ (Au)_x \rightarrow x(Au)_{x-1} + Au$$
$$(ii)\ (Au)_y + Au \rightarrow (Au)_{y+1} \text{ or } (Au)_y \rightarrow (Au)_{y-1} + Au$$
$$(iii)\ (Au)_z + Au \rightarrow (Au)_{z+1}$$

Then, the system reaches equilibrium. The concentration of Au^{3+} cations and the numbers of Au atoms remain constant before the depletion of smaller seeds, $(Au)_x$.[25] All nanoparticles grow at this step. Meanwhile, the cleavage of alkyl free radicals from SDS by UV-visible irradiation is still ongoing and the reduction of Au^{3+} cations to neutral Au atoms is continuous. The equilibrium of the system is finally lost due to the change of equilibrium concentration between Au^{3+} cations and the neutral Au atoms. However, the newly available neutral Au atoms make the medium size seeds, $(Au)_y$, quickly grow and eventually cross over the energy barrier (E_a), toward the stable surface-to-volume region. At this step, two groups of nanoparticles exist simultaneously, the larger ones $(Au)_{z+1}$ and smaller ones $(Au)_{y+1}$. After the depletion all available Au^{3+} cations, the supply of neutral Au atoms is no longer possible and the growth of Au nanoparticles stops.

3.3 Spectra data and deconvolution

The commercial software, PEAKFIT, was acquired to deconvolute and to fit the overlapping spectral bands of the Au nanoparticles. The mixed Gaussian and Lorentzian functions were selected to fit the spectral curves in this work. The R^2 value (coefficient of determination) was always larger than 0.995. The data were smoothed by a 25% Fourier filtering transform (FFT), and the baseline was subtracted before the spectral deconvolution. The principal assumption in this model is that each of the component peaks corresponds to a typical size of Au nanoparticles. The more deconvoluted the component peaks composing the absorption peak, the closer the final deconvoluted data to the real size distribution of Au nanoparticles. After the spectral deconvolution, all the overlapping peak areas and λ_{max} will be resolved, which presumably will have a ratio corresponding to the different sizes of Au nanoparticles existing in the samples.

A typical surface plasmon absorption spectrum of Au nanoparticles has a very broad absorbance band of interest, bandwidth = 450–600 nm, suggesting the possibility of overlapped components. Theoretically, the starting parameters of the deconvolution should be set by trial and error. Here, a spectrum was judged to have only four components, *i.e.* peak (x), peak (a), peak (b) and peak (c), as shown in Fig. 6. The shortest wavelength peak is peak (x) (λ_{max} ~455 nm) that comprises the shoulder of the Au^{3+} absorption peak (ranging from 280 to 460 nm with λ_{max} = 300 nm). Although, the concentration of Au^{3+} ions is very low in the solution, it can not be ignored. The other three peaks form the main parts of the peak area. The λ_{max} for the three peaks are, ~515 nm (peak (a)), ~535 nm (peak (b)) and ~560 nm (peak (c)), which represents the small size ($d \leq 5.1$ nm), medium size (5.1 nm $< d <$ 10.1 nm) and large size ($d \geq 10.1$ nm) Au nanoparticles. This classification is based on the size data derived from TEM images[29] and is theoretically supported by our previous study to categorize the size of nanoparticles into three main groups during the evolution progress of nanoparticles.[25]

The surface plasmon absorption spectra of D-8, D-10 and D-14 samples were selected for the spectra deconvolution analysis. The deconvolution results are listed in Table 1. Three tendencies of peak areas are observed in these deconvoluted data: (1) the total peak areas show an augmentation of

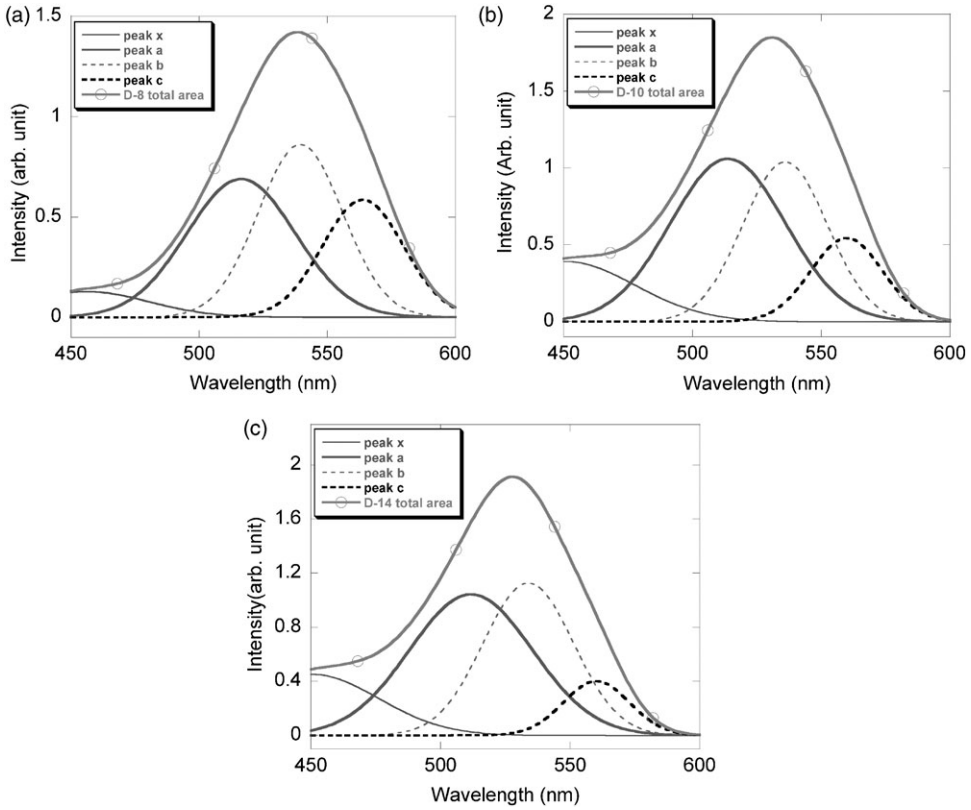

Fig. 6 Spectral deconvolution model for surface plasmon absorption spectra for (a) D-8, (b) D-10 and (c) D-14 samples, respectively. The shortest wavelength peak is peak (x) (λ_{max} ~455 nm) that comprises the shoulder of the Au^{3+} absorption peak. The λ_{max} for the other three peaks are, ~515 nm (peak (a)), ~535 nm (peak (b)) and ~560 nm (peak (c)), which represents the small size ($d \leq 5.1$ nm), medium size (5.1 nm $< d <$ 10.1 nm) and large size ($d \geq 10.1$ nm) Au nanoparticles.

38.94%, from D-8, D-10 to D-14. The augmentation of the total peak area implies that the whole amount of nanoparticles noticeably increases from D-8, D-10 to D-14, which is consistent with the results obtained from the TEM images. (2) The peak areas for peak (a) and peak (b) increase simultaneously, from D-8, D-10 to D-14. The increment for peak (a) is 68.60%, and the increment for peak (b) is 32.77%. The data verify that the increment of small nanoparticles numbers is obviously faster than that of medium size nanoparticles. (3) Peak (c) is the only one whose peak area decreases from D-8, D-10 to D-14. The peak area of peak (c) drops 21.24% from D-8 to D-14. Meanwhile, the increment of peak (a) is about 68.55% during the same time period. This variation in component peaks areas offers a clear evidence to elucidate the blue-shift phenomenon observed in the surface plasmon absorption spectra of the Au nanoparticles. The reason for the λ_{max} blue-shifting of the surface plasmon absorption from 545 nm (D-8) to 523 nm (D-14) is because the increment ratio of the small size nanoparticles (an increase of 68.55% of peak (a) area) is much faster than that of medium size nanoparticles (an increase of 32.77% of peak (b)) and the large nanoparticles even have an evident decrease of 21.24% of peak area during the nanoparticles evolution progress from D-8 to D-14. The large increase of the area ratio of peak (a) (λ_{max} between 516.36 and 509.0 nm), and the obvious decrease of the area ratio of peak (c) (λ_{max} between 563.9 and 557.7 nm) causes λ_{max} of the surface plasmon peak move from 545 nm (D-8) to 523 nm (D-14). If the number of small size nanoparticles can no longer be increased during the evolution, then the blue-shift phenomenon of the surface plasmon absorption peak will stop.

Table 1 The variation of peak[a] areas (and wavelength maximum/nm) in the D-8, D-10 and D-14 samples

Sample	Peak x	Peak a	Peak b	Peak c	Total area	$R^{2\,b}$
D-8	4.66 (455.98)	36.67 (516.36)	35.85 (539.45)	23.03 (563.9)	100.21	0.997
D-10	13.53 (454.6)	54.98 (512.40)	41.19 (533.3)	24.99 (558.0)	134.69	0.995
D-14	11.64 (451.19)	61.81 (509.0)	47.60 (531.8)	18.35 (557.7)	139.42	0.995

[a] The unit of peak area is arbitrary. [b] R^2 = coefficient of determination = 1 − (SSE/SSM), where SSE is the error sum of squares (measure of the variation of observed values around the regression line) and SSM is the mean sum of squares (measure of the variation of observed values around the mean).

4 Conclusion

A spectral deconvolution model has been proposed in the study to monitor the time-evolved kinetic-dependent nanocrystal growth mechanism of Au nanoparticles *via* a long-

wavelength UV-visible irradiation synthesis. TEM images were employed to calibrate the size of nanoparticles with different progress times. The appearance of the peak centered at 548 nm in the surface plasmon absorption spectra of D-5 samples confirms the successful nucleation of Au nanoparticles by long-wavelength UV-visible irradiation. The continuous λ_{max} blue-shift of the surface plasmon absorption peak from 548 nm (D-8 samples) to 523 nm (D-14 samples) is a result from the second growth progress of Au nanoparticles. The nanoparticles initiated from the first nucleation progress can mainly reach a size of 10–25 nm in diameter, but those accumulating from the second growth route mostly grow to the size of 3–5 nm.

Acknowledgements

The authors would like to thank Dr Wen-Jau Chen and Mr Jen-Ming Liu for their very useful help and discussions in TEM. C.-S. Y. is grateful for the financial support received from the National Science Council of Taiwan, ROC (under grant no. NSC 94-2113-M-415-006).

References

1 T. Teranishi and M. Miyake, *Chem. Mater.*, 1998, **10**, 594.
2 Y. Li, E. Boone and M. A. El-Sayed, *Langmuir*, 2002, **18**, 4921.
3 R. Narayanan and M. A. El-Sayed, *J. Am. Chem. Soc.*, 2003, **125**, 8340.
4 T. S. Ahmadi, Z. L. Wang, T. C. Green, A. Henglein and M. A. El-Sayed, *Science*, 1996, **272**, 1924.
5 R. Narayanan and M. A. El-Sayed, *J. Am. Chem. Soc.*, 2004, **126**, 7194.
6 J. Schulz, A. Roucoux and H. Patin, *Chem. Eur. J.*, 2000, **6**, 618.
7 T. K. Sau, A. Pal and T. Pal, *J. Phys. Chem. B*, 2001, **105**, 9266.
8 R. M. Crooks, M. Zhao, L. Sun, V. Chechik and L. K. Yeung, *Acc. Chem. Res.*, 2001, **34**, 181.
9 M. T. Reetz and W. J. Helbig, *J. Am. Chem. Soc.*, 1994, **116**, 7401.
10 M. T. Reetz and S. A. Quaiser, *Angew. Chem., Int. Ed. Engl.*, 1995, **34**, 2240.
11 K. Kurihara, J. Kizling, P. Stenius and J. H. Fengler, *J. Am. Chem. Soc.*, 1983, **105**, 2574.
12 M. Michaelis and A. J. Henglein, *J. Phys. Chem.*, 1992, **96**, 4719.
13 Y. Nagata, Y. Watanabe, S. Fujita, T. Dohmaru and S. J. Taniguchi, *J. Chem. Soc., Chem. Commun.*, 1992, 1620.
14 T. Fujimoto, S. Terauchi, H. Umehara, I. Kojima and W. Henderson, *Chem. Mater.*, 2001, **13**, 1057.
15 Y. Letichevsky, L. Sominski, J. C. Morenob and A. Gedanken, *New J. Chem.*, 2005, **29**, 1445.
16 P. V. Kamat, *J. Phys. Chem. B*, 2002, **106**, 7729.
17 R. Narayanan and M. A. El-Sayed, *J. Phys. Chem. B*, 2005, **109**, 12663.
18 M. B. Mohamed, V. Volkov, S. Link and M. A. El-Sayed, *Chem. Phys. Lett.*, 2000, **317**, 517.
19 P. V. Kamat, M. Flumiani and G. V. Hartland, *J. Phys. Chem. B*, 1998, **102**, 3123.
20 R. Jin, Y. W. Cao, C. A. Mirkin, K. L. Kelly, G. C. Schatz and J. G. Zheng, *Science*, 2001, **294**, 1901.
21 B. Shanghavi and P. V. Kamat, *J. Phys. Chem. B*, 1997, **101**, 7675.
22 H. Fujiwara, S. Yanagida and P. V. Kamat, *J. Phys. Chem. B*, 1999, **103**, 2589.
23 A. Henglein and D. Meisel, *Langmuir*, 1998, **14**, 7392.
24 S. Link and M. A. EL-Sayed, *J. Phys. Chem. B*, 1999, **103**, 4212.
25 C.-S. Yang, D. D. Awschalom and G. D. Stucky, *Chem. Mater.*, 2001, **13**, 594.
26 U. Kreibig and M. Vollmer, *Optical Properties of Metal Clusters*, Springer, Berlin, 1995.
27 C.-J. Chen, C.-S. Yang and X.-H. Lin, *Inorg. Chem. Commun.*, 2005, **8**, 836.
28 K. Okitsu, H. Bandow and Y. Maeda, *Chem. Mater.*, 1996, **8**, 315.
29 (*a*) The size boundary ($d \leq 5.1$ nm) for small nanoparticles is derived from D-5data (6.9 ± 1.8 nm; $6.9 - 1.8 = 5.1$). (*b*) The large size nanoparticles boundary ($d \geq 10.1$ nm) is based on the size distribution data of D-7 (8.2 ± 1.9 nm; $8.2 + 1.9 = 10.1$).